

Rate Splitting Multiple Access for Semi-Grant-Free Transmissions

Hongwu Liu, Theodoros A. Tsiftsis, Bruno Clerckx, Kyeong Jin Kim,
Kyung Sup Kwak, and H. Vincent Poor, *Life Fellow, IEEE*

Abstract

Enabled by hybrid grant-based (GB) and grant-free (GF) transmission techniques, GF users of internet of things (IoT) devices and massive machine-type communications (mMTC) meet opportunities to share wireless resources with GB users. In this paper, we propose a rate splitting multiple access (RSMA) strategy for an emerging semi-grant-free (SGF) transmission system to increase connectivity and reliability. In the proposed RSMA assisted SGF (RSMA-SGF) scheme, the GF users apply the rate splitting principle to realize distributed contentions and utilize transmit power most effectively for robust transmissions, meanwhile keeping themselves transparent to the GB user. Compared to existing non-orthogonal multiple access (NOMA) assisted SGF schemes, the RSMA-SGF scheme significantly decreases outage probability and achieves full multiuser diversity gain without restricting the GB and GF users' target rates to a limited value region. Exact expressions and asymptotic analysis for the outage probability are provided to facilitate the system performance evaluation of the proposed RSMA-SGF scheme. Computer simulation results clarify the superior outage performance of the RSMA-SGF scheme and verify the accuracy of the developed analytical results.

H. Liu is with the School of Information Science and Electrical Engineering, Shandong Jiaotong University, Jinan 250357, China (e-mail: liuhongwu@sdjtu.edu.cn).

T. A. Tsiftsis is with the School of Intelligent Systems Science and Engineering, Jinan University, Zhuhai 519070, China (e-mail: theo_tsiftsis@jnu.edu.cn).

K. J. Kim is with Mitsubishi Electric Research Laboratories, Cambridge, MA 02139 USA (e-mail: kkim@merl.com).

B. Clerckx is with the Department of Electrical and Electronic Engineering, Imperial College London, London, UK (e-mail: b.clerckx@imperial.ac.uk).

K. S. Kwak is with the Department of Information and Communication Engineering, Inha University, Incheon 22212, South Korea (e-mail: kskwak@inha.ac.kr).

H. V. Poor is with the Department of Electrical and Computer Engineering, Princeton University, Princeton, NJ 08544 USA (e-mail: poor@princeton.edu).

Index Terms

Rate splitting, multiple access, grant-free transmissions, outage probability.

I. INTRODUCTION

The explosive growth of internet-of-things (IoT) devices, intelligent robotics, and Industry 4.0 networks has created unprecedented demands for massive access, heterogeneous mobile traffic, and highly spectral efficient connectivity. On the road map of the fifth-generation (5G) evolution, enhanced mobile broadband (eMBB), ultra-reliable low latency communications (URLLC), and massive machine-type communications (mMTC) were standardized to facilitate the proliferation of the emerging application domains. Grant-free (GF) transmissions, which represent ubiquitous scenarios of beyond 5G URLLC and short packet traffic emitted by various sensors and massive IoT devices, have been envisioned to be a new air-interface trend for the next generation IoT [1]–[3]. Compared to conventional grant-based (GB) transmissions, where the amount of handshaking signalling could exceed the amount of data sent by devices, GF transmissions grant devices access without lengthy handshaking protocols [3]. Taking advantages of spectrum sharing from non-orthogonal multiple access (NOMA), semi-grant-free (SGF) transmissions opportunistically admitted GF users on the resource blocks occupied by the GB users in a multiplexing way, which surprisingly results in a higher spectrum efficiency than purely admitting GF or GB users [4], [5]. For NOMA assisted SGF (NOMA-SGF) transmissions, a series of the complicated handshaking process was omitted for granting latency-critical GF user, while collisions from GF users' contention can be elaborately relieved by using the NOMA philosophy¹ [5].

Taking into account the quality of service (QoS) requirements of GB users, GF users' contention needs to be carefully controlled for the NOMA-SGF schemes to prevent the system performance degradation to GB users. In particular, the system performance experienced by GB users should be the same as their counterparts in orthogonal multiplex access (OMA). It has been shown that the distributed contention protocol can ensure a fixed number of GF users to be granted access, while the open-loop protocol still suffers from user collisions as that in pure GF transmissions [5]. Furthermore, the equivalent received power at the base-station (BS) corresponding to GB transmission was broadcasted to GF users to facilitate distributed

¹In this paper, we only consider uplink SGF transmission scenarios. Therefore, all the mentioned NOMA and rate splitting multiple access (RSMA) in what follows are referred to the corresponding uplink schemes or scenarios.

contentions [6]. To maintain low-latency and high-reliability trade-off in addition to making GF users transparent to GB users, advanced code-domain or power-domain multiplexing and successive interference cancellation (SIC) techniques were exploited for the NOMA-SGF schemes [6]–[9]. Existing designs of the NOMA-SGF schemes largely depend on the SIC decoding order at the BS receiver and/or transmit power allocation. Based on the relative power levels, the hybrid SIC was applied to decode the desired signals, e.g., the admitted GF user’s signal can be decoded at the first stage or the second stage of the SIC to achieve the allowed maximum rate [10]. Associated with the hybrid SIC decoding order, transmit power allocation can be applied to improve the transmission reliability of the NOMA-SGF schemes [8], [9].

A. Related Work

The primary concept of NOMA-SGF was found in [4] and [5], respectively. In [4], the authors discussed the feasibility of applying NOMA to realize the SGF transmissions, including several NOMA solutions such as sparse-code multiple access (SCMA), power-domain NOMA, pattern-division multiple access (PDMA), and interleave division multiple access (IDMA). Two basic NOMA-SGF schemes were firstly proposed using the power-domain NOMA philosophy without causing too much performance degradation to GB users [5]. Considering stochastic geometry in outage performance analysis, an accurate interference threshold was adopted for granting GF users [7], [11]. In [6] and [10], the authors proposed to use the hybrid SIC decoding order to ensure that GB user can experience the same system performance as in OMA, meanwhile aiming at improving the transmission reliability for the granted GF user. Adaptive power allocation methods were designed for the NOMA-SGF schemes using the fixed SIC decoding order [9] and hybrid SIC decoding order [8], respectively. In [12], the cognitive radio (CR) principle was applied to manage interference from GF users to a selected GB user. For the tactile IoT network where the NOMA-SGF is applied, the authors of [13] proposed a solution to the joint channel assignment and power allocation problem. The ergodic rate analysis was provided in [14] and most recently a multi-agent deep reinforcement learning algorithm was proposed to optimize the transmit power pool for the NOMA-SGF systems [15].

B. Motivations and Contributions

For multiple access channels (MACs), rate splitting (RS) was proposed to achieve the capacity region [16]. Considering that uplink NOMA scenarios can be regarded as MACs, rate splitting

multiple access (RSMA) strategies were applied to achieve the capacity region for uplink NOMA transmissions [17], [18]. Motivated by the CR principles, we developed the adaptive power allocation method for the RSMA to guarantee the QoS requirements of the paired uplink users [18]. For the uplink single-input multiple-output (SIMO) NOMA systems, the RS scheme was designed to ensure max-min fairness among the NOMA users [19]. The sum-rate of the uplink MACs was maximized with the aid of the RSMA by adjusting the users' transmit power and the BS's decoding order [20]. Very recently, the RS techniques were applied for multiple access in the uplink aerial networks [21].

In this paper, we adopt the same uplink SGF transmission scenario originally introduced in [5] and lately investigated in [6]. An RS strategy is proposed for the SGF transmission system to realize the RSMA assisted SGF (RSMA-SGF) scheme. We apply the RS techniques at the GF users not only for the distributed contentions but also for the SGF transmissions with the aim of improving the transmission reliability for the admitted GF user.

The main contributions of this paper are summarized as follows:

- We propose RSMA-SGF and contrast with NOMA-SGF for uplink SGF network deployments. The GF users apply the RS strategy to calculate their achievable rates and determine the corresponding back-off time for the distributed contentions. By using the RS strategy, the admitted GF user's transmission is transparent to the GB user, while the transmit power of the admitted GF user is effectively exploited to enhance its transmission reliability.
- We derive exact expression for the outage probability and its high signal-to-noise ratio (SNR) approximation to facilitate the evaluation of the outage performance for the proposed RSMA-SGF scheme. The analytical results reveal that the RSMA-SGF scheme can achieve the full multiuser diversity gain without restricting the GB and GF users' target rates to a limited value region, which is more robust than the existing NOMA-SGF schemes.
- We evaluate the accuracy of the developed analytical results and high SNR approximations via computer simulations. The impact of several system parameters on the outage performance is revealed. Compared to existing NOMA-SGF schemes, the proposed RSMA-SGF scheme achieves the best outage performance over the existing NOMA-SGF schemes. In addition, due to the capability of RSMA to achieve the capacity region of MACs, the proposed RSMA-SGF scheme works well for a wider region of the target rates than the existing NOMA-SGF schemes.

The remainder of this paper is organized as follows: Section II and Section III present the

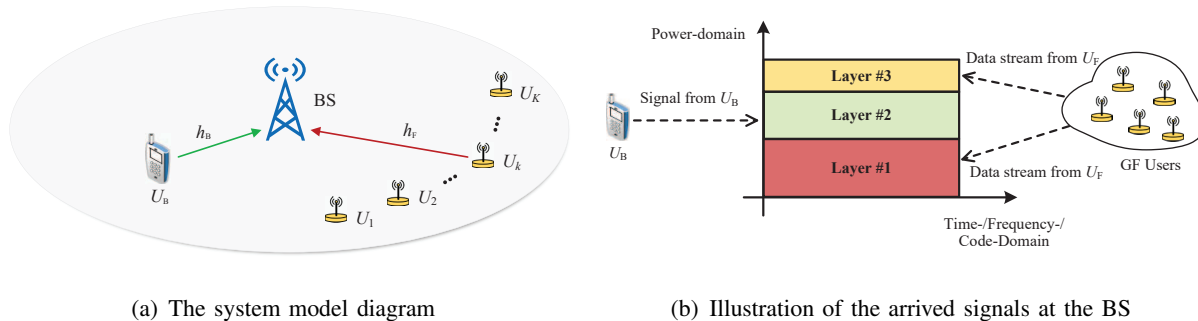


Fig. 1. An illustration of the considered NOMA-SGF system and signal model.

system model and RSMA-SGF scheme, respectively; In Section IV, the outage performance of the proposed RSMA-SGF scheme is analyzed and the high SNR approximation for the outage probability is presented; In Section V, simulation results are presented for corroborating the superior outage performance of the RSMA-SGF scheme and Section VI summarizes this work.

II. SYSTEM MODEL

We consider the uplink scenario in an SGF transmission system, as depicted in Fig. 1(a), where K GF users, $\{U_1, U_2, \dots, U_K\}$, compete to be paired with a GB user, U_B , for uplink transmissions. To ensure that the admission of the GF users do not cause too much interference to the GB user, we consider that only a single user is grant access simultaneously with the GB user [6]. After the user contention and access admission, the paired GB and GF users share the same resource block for their uplink transmissions. Denote the GB user’s channel by h_B and the k th ($k \in \{1, 2, \dots, K\}$) GF user’s channel by h_k , which are modeled as independent and identically distributed (i.i.d.) Rayleigh fading. Without loss of generality, we assume that the GF users’ channel gains are ordered as

$$|h_1|^2 \leq |h_2|^2 \leq \dots \leq |h_K|^2 \tag{1}$$

to facilitate the system performance analysis. It should be noted that the above ordering information is unavailable to the BS and all the GF users. In addition, we assume that the GB and GF users have the knowledge of their own CSI, respectively, and the BS has acquired the knowledge of the CSI of the GB user as well as its transmit power, P_B . In addition, the CSI of the admitted GF user is not required to be known at the BS prior to transmission. The detailed CSI acquisition procedure will be discussed in Subsection B of Section III. We assume that the

channels follow a statistical fading, i.e., the channel fading coefficients keep constant during a single transmission block and can vary from one transmission block to another independently.

III. RATE SPLITTING MULTIPLE ACCESS ASSISTED SEMI-GRANT-FREE SCHEME

In the proposed RSMA-SGF scheme, the grant access of the GF user is transparent to the GB user. Therefore, we only consider that the RS is carried out at the GF user and the RSMA-SGF scheme is designed to improve the achievable rate of the GF user over its counterpart in a NOMA-SGF scenario where the RS is not applied.

A. Signal Model

We assume that the GF user $U_F \in \{U_1, U_2, \dots, U_K\}$ is admitted to transmit its signal x_F being paired with the GB user. Before the uplink transmission, U_F splits its signal x_F into two streams $x_{F,1}$ and $x_{F,2}$. The transmit power of the admitted GF user, P_F , is allocated for the two streams according to $\tilde{x}_F = \sqrt{\alpha P_F} x_{F,1} + \sqrt{(1-\alpha)P_F} x_{F,2}$, where α is the transmit power allocation factor satisfying $0 \leq \alpha \leq 1$. In each transmission block, the paired GB and GF users transmit their signals simultaneously to the BS and the received signal at the BS can be written as

$$y = \sqrt{P_B} h_B x_B + \sqrt{\alpha P_F} h_F x_{F,1} + \sqrt{(1-\alpha)P_F} h_F x_{F,2} + w, \quad (2)$$

where x_B is the GB user's signal, $h_F \in \{h_1, h_2, \dots, h_K\}$ is the channel of the admitted GF user, and w is additive white Gaussian noise (AWGN) with zero mean and unit variance. We assume that the transmitted signal $x_i \in \{x_B, x_F, x_{F,1}, x_{F,2}\}$ is obtained by independent coding with Gaussian code book satisfying $\mathbb{E}\{|x_i|^2\} = 1$. As an example, we give an illustration in Fig. 1(b) for the arrived power levels at the BS, where Layers #1, #2, and #3 correspond to $\sqrt{\alpha P_F} h_F x_{F,1}$, $\sqrt{P_B} h_B x_B$, and $\sqrt{(1-\alpha)P_F} h_F x_{F,2}$, respectively. In a nutshell, Layers #1, #2, and #3 are superimposed in the power-domain according to the RSMA philosophy [16].

In the signal model of (2), the RS is carried out only for $0 < \alpha < 1$. For the case of $\alpha = 0$ or $\alpha = 1$, the admitted GF user transmits the signal $x_{F,2} = x_F$ or $x_{F,1} = x_F$ without operating in the RS mode. Consequently, the SIC decoding modes at the BS are determined by the different values of α , which are discussed as follows:

- For the case of $0 < \alpha < 1$, the decoding order $x_{F,1} \rightarrow x_B \rightarrow x_{F,2}$ is applied at the BS to recover the desired signals, $x_{F,1}$, x_B , and $x_{F,2}$, sequentially [18]. In other words, the GB user's signal is decoded in the second stage of the SIC processing, whereas the admitted

GF user's streams are decoded in the first and third stages, respectively. Once the streams $x_{F,1}$ and $x_{F,2}$ are recovered successfully, all the information transmitted by the GF user can be retrieved at the BS. In this case, the achievable rates for transmitting $x_{F,1}$, x_B , and $x_{F,2}$ can be expressed as

$$R_{F,1} = \log_2 \left(1 + \frac{\alpha P_F |h_F|^2}{P_B |h_B|^2 + (1 - \alpha) P_F |h_F|^2 + 1} \right), \quad (3)$$

$$R_B = \log_2 \left(1 + \frac{P_B |h_B|^2}{(1 - \alpha) P_F |h_F|^2 + 1} \right), \quad (4)$$

and

$$R_{F,2} = \log_2 (1 + (1 - \alpha) P_F |h_F|^2), \quad (5)$$

respectively. For the admitted GF user, its achievable rate is given by $R_F = R_{F,1} + R_{F,2}$.

- For the case of $\alpha = 0$, since the admitted GF user only transmits $x_{F,2} = x_F$, the decoding order $x_B \rightarrow x_F$ is applied at the BS to recover the desired signals, x_B and x_F , sequentially. The achievable rates of the paired GB and GF users are given by $R_B = \log_2 \left(1 + \frac{P_B |h_B|^2}{P_F |h_F|^2 + 1} \right)$ and $R_F = \log_2 (1 + P_F |h_F|^2)$, respectively.
- For the case of $\alpha = 1$, the admitted GF user only transmits $x_{F,1} = x_F$, the decoding order $x_F \rightarrow x_B$ is applied at the BS to recover the desired signals, x_F and x_B , sequentially. The achievable rates of the paired GF and GB users are given by $R_F = \log_2 \left(1 + \frac{P_F |h_F|^2}{P_B |h_B|^2 + 1} \right)$ and $R_B = \log_2 (1 + P_B |h_B|^2)$, respectively.

B. RSMA-SGF Scheme

Prior to admission, the BS broadcasts an interference threshold τ to all the K GF users to realize the distributed contention. Recalling that the GB user's signal needs to be decoded correctly in the second stage of the SIC processing for $0 < \alpha < 1$, it requires that $\log_2 \left(1 + \frac{P_B |h_B|^2}{(1 - \alpha) P_F |h_F|^2 + 1} \right) \geq \hat{R}_B$ with \hat{R}_B denoting the GB user's target transmission rate. Therefore, the interference threshold is designed as $\tau = \max \{0, \hat{\tau} (|h_B|^2)\}$, where $\hat{\tau} (|h_B|^2) = \frac{P_B |h_B|^2}{2^{\hat{R}_B} - 1} - 1$ denotes the maximum interference power allowed by the GB user's QoS requirements. In the proposed RSMA-SGF scheme, the GF user that achieves the allowed maximum R_F will be admitted for transmissions.

The admission procedure of the RSMA-SGF scheme consists of the following steps:

- The BS broadcasts pilot signal to assist the GB and GF users to estimate their channels.
- The GB user feeds back its transmission power P_B and CSI h_B to the BS.

- The BS calculates the interference threshold τ and broadcasts it to all the K GF users.
- Each GF user calculates its achievable rate and determines the associated backoff time.
- Through the distributed contention, the GF user that has the minimum backoff time is admitted.

According to the relationship between $P_F |h_k|^2$ and τ , the K GF users are categorized into two groups and determine their achievable rates as in the following:

- Group I: In this group, the received signal power at the BS corresponding to the U_k 's transmission is less than or equal to τ , i.e., $P_F |h_k|^2 \leq \tau$. To achieve the allowed maximum transmission rate, U_k does not conduct RS and transmits its signal directly by setting $\alpha = 0$. At the BS receiver, the decoding for the GB user's signal is carried out at the first stage of the SIC processing, while the decoding for the U_k 's signal is carried out at the second stage, which yields the achievable rate $R_{I,k} = \log_2(1 + P_F |h_k|^2)$ for the U_k 's transmission.
- Group II: In this group, the received signal power at the BS corresponding to the U_k 's transmission is larger than τ , i.e., $P_F |h_k|^2 > \tau$. For the GF user U_k in this group, RS is carried out for its transmission by setting $\alpha = 1 - \frac{\tau}{P_F |h_k|^2}$, which yields the achievable rate $\log_2(1 + \tau)$ for transmitting $x_{F,2}$. Substituting $\alpha = 1 - \frac{\tau}{P_F |h_k|^2}$ into (3), the achievable rate for transmitting $x_{F,1}$ can be determined and the total achievable rate for the U_k 's transmission can be written as $R_{II,k} = \log_2\left(1 + \frac{P_F |h_k|^2 - \tau}{P_B |h_B|^2 + \tau + 1}\right) + \log_2(1 + \tau)$.

Based on the above discussions, the achievable rate of U_k is given by

$$R_k = \begin{cases} R_{I,k}, & P_F |h_k|^2 \leq \tau \\ R_{II,k}, & P_F |h_k|^2 > \tau \end{cases}, \quad (6)$$

In order to guarantee that the GB user can attain the same outage performance as in OMA, the admitted GF user in Group II is allowed to transmit its signal only when $R_k \geq \hat{R}_F$, where \hat{R}_F denotes the target transmissions rate of all the GF users; Otherwise, the GF user in Group II keeps silent during the transmissions. In this way, the failure of decoding $x_{F,1}$ in the first stage of the SIC processing can be avoided, while the GB user still experiences the same performance as in OMA. To realize distributed contention, the backoff time of U_k is set to be inversely proportional to its achievable rate [22]–[24]. Thus, the GF user with the largest R_k will be granted access in a distributed manner.

Remark 1: Since $R_{I,k}$ is monotonically increasing with respect to $|h_k|^2$ while $|h_1|^2 \leq |h_2|^2 \leq \dots \leq |h_K|^2$, the GF user having the largest $|h_k|^2$ in Group I will be granted access if Group II

is empty. Similarly, the GF user having the largest $|h_k|^2$ in Group II will be granted access if Group I is empty. When both Group I and Group II are not empty, a single user has the chance of being granted access since that $R_{\text{II},k} > R_{\text{I},k}$ always holds based on the fact $R_{\text{I},k} \leq \log_2(1 + \tau)$. Therefore, in the proposed RSMA-SGF scheme, only a single user who has the largest $|h_k|^2$ will be granted access and the backoff time of all the K GF users can be directly set to be inversely proportional to their channel gains, respectively.

Remark 2: If all the GF users are in Group I under the condition that $\tau > 0$, the admitted GF user will set $\alpha = 0$. When $\tau = 0$ occurs, i.e., the GB user cannot guarantee its QoS requirements, all the GF users are in Group II and the admitted GF user will set $\alpha = 1$. For the cases of $\alpha = 0$ and $\alpha = 1$, the admitted GF user does not carry out the RS for the transmissions and transmits its signal x_{F} directly. Besides, $R_{\text{II},k} = \log_2 \left(1 + \frac{P_{\text{F}}|h_k|^2}{P_{\text{B}}|h_{\text{B}}|^2 + 1} \right)$ when $\tau = 0$ occurs.

Remark 3: If a GF user in Group II is to be admitted, it keeps silent during the transmissions when $R_{\text{F}} < \hat{R}_{\text{F}}$. In this case, although the GF user suffers an outage event due to its silent behavior, the GB user occupies the granted resource blocks solely, i.e., the GB user transmits its signal as in an OMA scenario. Recalling that the admitted GF user in Group I also does not affect the outage performance of the GB user compared to that in OMA, the proposed RSMA-SGF scheme results in the same outage performance for the GB user as in OMA.

IV. OUTAGE PERFORMANCE

In the proposed RSMA-SGF scheme, the admission of the GF user is transparent to the GB user whose performance is the same as in OMA. Thus, we mainly focus on the outage performance of the admitted GF user. In this section, we derive closed-form analytical expression for the outage probability of the admitted GF user. Then, its asymptotic outage performance is investigated in the high SNR region.

To characterize the outage performance, we denote the event that there are k GF users in Group I by E_k , which can be explicitly expressed by

$$E_k = \left\{ |h_k|^2 \leq \frac{\tau}{P_{\text{F}}}, |h_{k+1}|^2 > \frac{\tau}{P_{\text{F}}} \right\} \quad (7)$$

for $1 \leq k \leq K - 1$. Furthermore, we denote the two extreme events with no user in Group I and Group II by $E_0 = \left\{ |h_1|^2 > \frac{\tau}{P_{\text{F}}} \right\}$ and $E_K = \left\{ |h_K|^2 < \frac{\tau}{P_{\text{F}}} \right\}$, respectively.

When the event E_k ($1 \leq k \leq K - 1$) occurs, Group II contains the $K - k$ GF users among them who has the largest achievable rate will be admitted. For this case, the achievable rate of

the admitted GF user is given by $\max\{R_{\text{II},m}, k < m \leq K\}$. If $\max\{R_{\text{II},m}, k < m \leq K\} < \hat{R}_{\text{F}}$, an outage event happens for E_k . As such, the outage events for E_0 and E_K can be defined. Therefore, the outage probability experienced by the admitted GF user can be expressed as

$$P_{\text{out}} = \Pr\left(E_0, \max\{R_{\text{II},m}, 1 \leq m \leq K\} < \hat{R}_{\text{F}}\right) + \sum_{k=1}^{K-1} \Pr\left(E_k, \max\{R_{\text{II},m}, k < m \leq K\} < \hat{R}_{\text{F}}\right) + \Pr\left(E_K, \max\{R_{\text{I},m}, 1 \leq m \leq K\} < \hat{R}_{\text{F}}\right). \quad (8)$$

Because the grant-free users' channel gains are ordered as in (1) while $R_{\text{I},k}$ and $R_{\text{II},k}$ are monotonically increasing with respect to $|h_k|^2$, the outage probability can be simplified as follows:

$$P_{\text{out}} = \Pr\left(E_0, R_{\text{II},K} < \hat{R}_{\text{F}}\right) + \sum_{k=1}^{K-1} \Pr\left(E_k, R_{\text{II},K} < \hat{R}_{\text{F}}\right) + \Pr\left(E_K, R_{\text{I},K} < \hat{R}_{\text{F}}\right). \quad (9)$$

Define $\epsilon_{\text{B}} \triangleq 2^{\hat{R}_{\text{B}}} - 1$, $\epsilon_{\text{F}} \triangleq 2^{\hat{R}_{\text{F}}} - 1$, $\eta_{\text{B}} \triangleq \frac{\epsilon_{\text{B}}}{P_{\text{B}}}$, and $\eta_{\text{F}} \triangleq \frac{\epsilon_{\text{F}}}{P_{\text{F}}}$, we have

$$\tau = \max\left\{0, \frac{|h_{\text{B}}|^2}{\eta_{\text{B}}} - 1\right\} = 0 \quad (10)$$

when $|h_{\text{B}}|^2 < \eta_{\text{B}}$. Therefore, the outage probability experienced by the admitted GF user can be rewritten as follows:

$$P_{\text{out}} = \underbrace{\Pr\left(E_0, |h_{\text{B}}|^2 > \eta_{\text{B}}, R_{\text{II},K} < \hat{R}_{\text{F}}\right)}_{Q_0} + \sum_{k=1}^{K-1} \underbrace{\Pr\left(E_k, |h_{\text{B}}|^2 > \eta_{\text{B}}, R_{\text{II},K} < \hat{R}_{\text{F}}\right)}_{Q_k} + \underbrace{\Pr\left(E_K, |h_{\text{B}}|^2 > \eta_{\text{B}}, R_{\text{I},K} < \hat{R}_{\text{F}}\right)}_{Q_K} + \underbrace{\Pr\left(|h_{\text{B}}|^2 < \eta_{\text{B}}, R_{\text{II},K} < \hat{R}_{\text{F}}\right)}_{Q_{K+1}}. \quad (11)$$

For the proposed RSMA-SGF scheme, the following theorem provides an exact expression for the outage probability experienced by the admitted GF user.

Theorem 1: Assume that $K \geq 2$, the outage probability experienced by the admitted GF user is given by

$$P_{\text{out}} = \frac{\varphi_0}{K(K-1)} \sum_{\ell=0}^K \binom{K}{\ell} (-1)^\ell \mu_1 \nu(0, \mu_2) + \sum_{k=1}^{K-2} \varphi_k \sum_{n=0}^{K-k} \binom{K-k}{n} (-1)^n \sum_{\ell=0}^k \binom{k}{\ell} (-1)^\ell e^{\frac{\ell}{P_{\text{F}}}} \mu_3 \nu(\ell, \mu_4) + \frac{\varphi_0}{K-1} \sum_{\ell=0}^{K-1} \binom{K-1}{\ell} (-1)^\ell e^{\frac{\ell}{P_{\text{F}}}} \left(e^{\frac{1}{P_{\text{F}}}} \nu(\ell, \mu_5) - e^{-\frac{\epsilon_{\text{B}} + \epsilon_{\text{F}} + \epsilon_{\text{B}} \epsilon_{\text{F}}}{P_{\text{F}}}} \nu(\ell, \mu_6) \right)$$

$$\begin{aligned}
& + \sum_{\ell=0}^K \binom{K}{\ell} (-1)^\ell e^{\frac{\ell}{P_F}} \nu(\ell, 0) + (1 - e^{-\eta_F})^K e^{-\eta_B(1+\epsilon_F)} \\
& + \sum_{\ell=0}^K \binom{K}{\ell} (-1)^\ell e^{-\ell\eta_F} \frac{1 - e^{-(1+\ell\eta_F P_B)\eta_B}}{1 + \ell\eta_F P_B}, \tag{12}
\end{aligned}$$

where $\mu_1 = e^{\frac{K-\ell(1+\epsilon_B)(1+\epsilon_F)}{P_F}}$, $\mu_2 = \frac{K-\ell}{P_F\eta_B} - \frac{P_B\ell}{P_F}$, $\mu_3 = e^{\frac{K-k-n(1+\epsilon_B)(1+\epsilon_F)}{P_F}}$, $\mu_4 = \frac{K-k-n}{P_F\eta_B} - \frac{nP_B}{P_F}$, $\mu_5 = \frac{1}{P_F\eta_B}$, $\mu_6 = -\frac{P_B}{P_F}$, $\varphi_0 = \frac{K!}{(K-2)!}$, $\varphi_k = \frac{K!}{k!(K-k)!}$ for $1 \leq k \leq K-2$, and

$$\nu(\ell, \mu) = \begin{cases} \epsilon_F \eta_B, & \text{if } \mu = -1 - \frac{\ell}{P_F\eta_B}, \\ \frac{e^{-\eta_B(\frac{\ell}{P_F\eta_B} + \mu + 1)} - e^{-\eta_B(1+\epsilon_F)(\frac{\ell}{P_F\eta_B} + \mu + 1)}}{\frac{\ell}{P_F\eta_B} + \mu + 1}, & \text{otherwise.} \end{cases} \tag{13}$$

Proof: See Appendix A. ■

Remark 4: Recalling the relationships between the upper and lower bounds on the channel gains for deriving Q_k ($0 \leq k \leq K$) as in Appendix A, the corresponding upper bound is always larger than the corresponding lower bound when $|h_B|^2 < \eta_B(1 + \epsilon_F)$ without requiring any additional constraints on ϵ_B and ϵ_F . Therefore, the derived expression in Theorem 1 for the outage probability holds for all the feasible values of ϵ_B and ϵ_F . On the contrary, the outage probability expression derived for the NOMA-SGF scheme as in [6] holds only for $\epsilon_B\epsilon_F < 1$, which restricts the target rate pair (\hat{R}_B, \hat{R}_F) under which the outage floor can be avoided. In the case of $\epsilon_B\epsilon_F \geq 1$, the admitted GF user in the NOMA-SGF scheme exhibits an outage floor, whereas this is not the case in the proposed RSMA-SGF scheme. As it will be verified by the simulation results in Section V, the RSMA-SGF scheme outperforms the NOMA-SGF scheme in terms of the outage probability for all the feasible values of ϵ_B and ϵ_F .

Remark 5: Due to the fact that different Q_k s involve different order statistics, the resulted outage probability expression shown in Theorem 1 is complicated. For example, Q_0 is a function of three channel gains, $|h_B|^2$, $|h_1|^2$, and $|h_K|^2$, whereas Q_k ($1 \leq k \leq K-2$) is a function of four channel gains, $|h_B|^2$, $|h_k|^2$, $|h_{k+1}|^2$, and $|h_K|^2$. Although $|h_B|^2$ is independent of $|h_k|^2$ ($1 \leq k \leq K$), $|h_k|^2$ s are dependent order statistics with $1 \leq k \leq K$, which makes the expression even more involved. Fortunately, insightful approximations at high SNR can be obtained as shown in Theorem 2.

When there is only a single GF user in the considered system, it is paired with the GB user without the distributed contention. In this case, the outage probability experienced by the single

GF user can be written as

$$P_{\text{out}} = \Pr\left(|h_{\text{B}}|^2 > \eta_{\text{B}}, |h_{\text{I},1}|^2 > \frac{\tau}{P_{\text{F}}}, R_{\text{II},1} < \hat{R}_{\text{F}}\right) + \Pr\left(|h_{\text{B}}|^2 > \eta_{\text{B}}, |h_{\text{I},1}|^2 < \frac{\tau}{P_{\text{F}}}, R_{\text{I},1} < \hat{R}_{\text{F}}\right) \\ + \Pr\left(|h_{\text{B}}|^2 < \eta_{\text{B}}, R_{\text{II},1} < \hat{R}_{\text{F}}\right). \quad (14)$$

By applying the similar steps as in the proof for Theorem 1, the outage probability experienced by a single GF user can be obtained straightforwardly as shown in the following corollary.

Corollary 1: Assume that $K = 1$, the outage probability experienced by the single GF user can be expressed as follows:

$$P_{\text{out}} = 1 - e^{-\frac{\epsilon_{\text{B}} + \epsilon_{\text{F}} + \epsilon_{\text{B}}\epsilon_{\text{F}}}{P_{\text{F}}}} \nu(0, \mu_6) - e^{-\eta_{\text{F}} - \eta_{\text{B}}(1 + \epsilon_{\text{F}})} - \frac{e^{-\eta_{\text{F}}}(1 - e^{-\eta_{\text{B}} - \epsilon_{\text{B}}\eta_{\text{F}}})}{1 + P_{\text{B}}\eta_{\text{F}}}. \quad (15)$$

Remark 6: For the case of the single GF user, the above expression for the outage probability also holds for all the feasible values of ϵ_{B} and ϵ_{F} . As a result, the single GF user does not experience an outage floor when $\epsilon_{\text{B}}\epsilon_{\text{F}} \geq 1$, which will be verified by the simulation results in Section V.

Theorem 2: Assume that $K \geq 2$ and $P_{\text{B}} = P_{\text{F}} \rightarrow \infty$, the outage probability experienced by the admitted GF user can be approximated at high SNR as follows:

$$P_{\text{out}} \approx \frac{\varphi_0 \epsilon_{\text{B}} (1 + \epsilon_{\text{B}})^K}{P_{\text{F}}^{K+1} K (K-1)} \sum_{\ell=0}^K \binom{K}{\ell} \frac{(-1)^\ell}{\ell+1} \left((1 + \epsilon_{\text{F}})^{K+1} - (1 + \epsilon_{\text{F}})^{K-\ell} \right) \\ + \frac{\varphi_k \epsilon_{\text{B}} (1 + \epsilon_{\text{B}})^{K-k} (-1)^k}{P_{\text{F}}^{K+1}} \sum_{n=0}^{K-k} \binom{K-k}{n} (-1)^n (1 + \epsilon_{\text{F}})^{K-k-n} \\ \times \sum_{\ell=0}^k \binom{k}{\ell} (-1)^\ell \frac{(1 + \epsilon_{\text{F}})^{n+\ell+1} - 1}{n + \ell + 1} + \frac{\varphi_0 \epsilon_{\text{B}} \epsilon_{\text{F}}^K (1 + \epsilon_{\text{B}})(1 + \epsilon_{\text{F}})}{P_{\text{F}}^{K+1} K (K-1)} \\ - \frac{\varphi_0 \epsilon_{\text{F}}^K (\epsilon_{\text{B}}^{-1} + 1)(K(1 + \epsilon_{\text{F}}) + 1)}{P_{\text{F}}^{K+1} K (K-1)(K+1)} + \frac{\epsilon_{\text{B}} \epsilon_{\text{F}}^{K+1}}{(K+1)P_{\text{F}}^{K+1}} + \frac{\epsilon_{\text{F}}^K}{P_{\text{F}}^K} - \frac{\epsilon_{\text{B}} \epsilon_{\text{F}}^K (1 + \epsilon_{\text{F}})}{P_{\text{F}}^{K+1}} \\ + \frac{\epsilon_{\text{F}}^K ((1 + \epsilon_{\text{B}})^{K+1} - 1)}{P_{\text{F}}^{K+1}(K+1)} - \frac{\epsilon_{\text{F}}^K ((\epsilon_{\text{B}}(K+1) - 1)(1 + \epsilon_{\text{B}})^{K+1} + 1)}{P_{\text{F}}^{K+2}(K+2)(K+1)}. \quad (16)$$

Proof: See Appendix B. ■

From the results in Theorem 2, we can see that there is one term in P_{out} being proportional to $\frac{1}{P_{\text{F}}^K}$, while the other terms are proportional to $\frac{1}{P_{\text{F}}^{K+1}}$ or $\frac{1}{P_{\text{F}}^{K+2}}$. Therefore, we have the following corollary.

Corollary 2: Assuming that $K \geq 2$ and $P_{\text{F}} = P_{\text{B}} \rightarrow \infty$, the outage probability experienced by the GF user can be further approximated as $\frac{\epsilon_{\text{F}}^K}{P_{\text{F}}^K}$ and a diversity gain of K is achievable for the proposed RSMA-SGF scheme.

As a result, the RSMA-SGF scheme can achieve the diversity gain K irrespective of $\epsilon_B \epsilon_F \geq 1$.

Corollary 3: Assume that $K = 1$, the outage probability experienced by the single GF user can be approximated as follows:

$$P_{\text{out}} \approx \epsilon_F P_F^{-1}. \quad (17)$$

Proof: See Appendix C. ■

Remark 7: Corollaries 2 and 3 demonstrate that the proposed RSMA-SGF scheme not only avoids an outage floor, but also ensures an achievable diversity gain proportional to the number of the GF users who participate in the distributed contention. In addition, the diversity gain is achievable irrespective of the values of ϵ_B and ϵ_F , whereas the existing QoS-Guaranteed SGF (QoS-SGF) scheme requires that $\epsilon_B \epsilon_F < 1$ to achieve the diversity gain [6]. Thus, compared to the QoS-SGF scheme, the RSMA-SGF scheme provides a wide ranges of target rates to achieve the diversity gain.

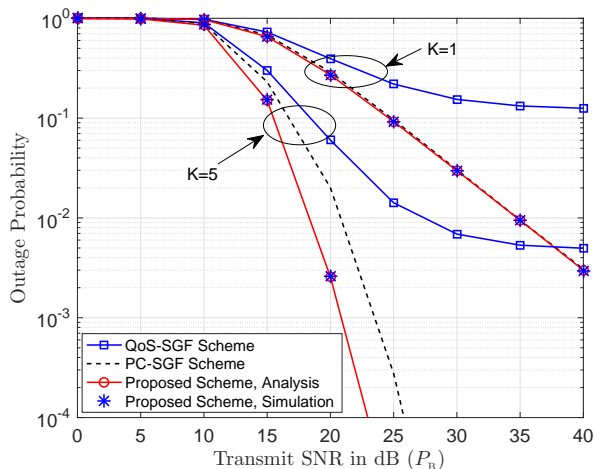
Corollary 4: The RSMA-SGF scheme avoids an outage floor without restricting the target rates to a limited value region.

Proof: See Appendix D. ■

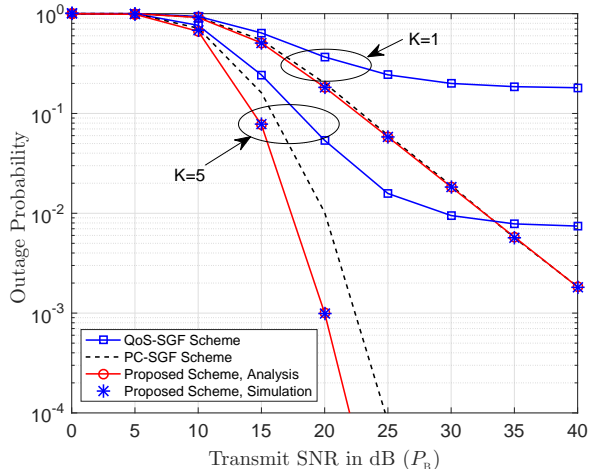
V. SIMULATION RESULTS

In this section, we present computer simulation results to verify the accuracy of the developed analytical results and clarify the outage performance achieved by the proposed RSMA-SGF scheme. For the purpose of comparison, two existing NOMA-SGF schemes, namely, the QoS-SGF scheme [6] and power control-aided SGF (denoted by PC-SGF) scheme [8], are chosen as the benchmarking schemes. It is noted that the hybrid SIC decoding order was applied in both the QoS-SGF and PC-SGF schemes to enhance the outage performance [6], [8]. In addition, the optimized power control was adopted in the PC-SGF scheme [8]. In the simulation, the unit for measuring the transmission data rate and target rate is bits per channel use (BPCU).

In Fig. 2, the outage performance achieved by the proposed RSMA-SGF scheme is compared with the QoS-SGF and PC-SGF schemes for various choices of the target rate pair $\{\hat{R}_B, \hat{R}_F\}$. In particular, we set $P_F = \frac{P_B}{10}$ in Fig. 2 to reflect the scenarios in which the channel conditions of the GF users are weaker than that of the GB user. In Figs. 2(a) and 2(b), we set the target rate pairs as $\{\hat{R}_B = 1.5 \text{ BPCU}, \hat{R}_F = 2 \text{ BPCU}\}$ and $\{\hat{R}_B = 2 \text{ BPCU}, \hat{R}_F = 1.5 \text{ BPCU}\}$, respectively, to indicate that the GB user has a larger or smaller target rate than that of the GF users. From



(a) $\hat{R}_B = 1.5$ BPCU and $\hat{R}_F = 2$ BPCU



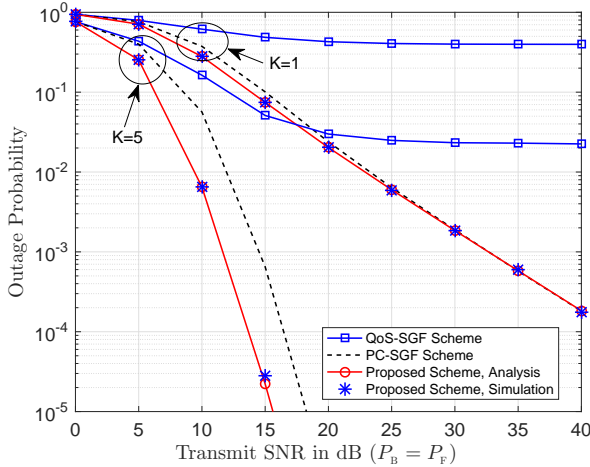
(b) $\hat{R}_B = 2$ BPCU and $\hat{R}_F = 1.5$ BPCU

Fig. 2. Outage probability comparison of the SGF schemes for various target rate settings.

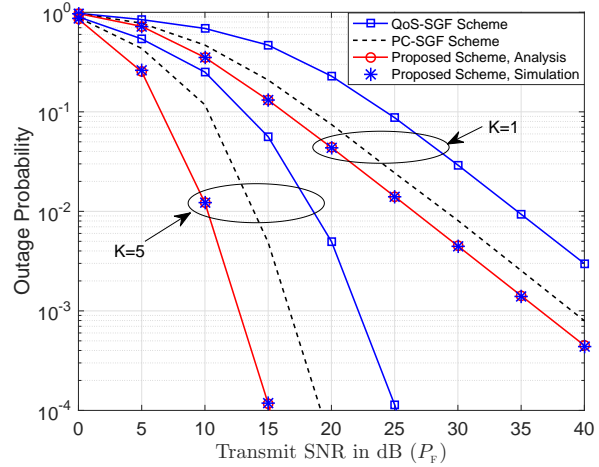
Figs. 2(a) and 2(b), we can see that the proposed RSMA-SGF scheme achieves the best outage performance among three schemes for both $K = 1$ and $K = 5$. In addition, we can see that the QoS-SGF scheme causes the floors on the outage probability. The reason for this phenomenon is that QoS-Scheme requires $\epsilon_B \epsilon_F < 1$ to achieve its superior outage performance, whereas we set $\epsilon_B \epsilon_F > 1$ in Figs. 2(a) and 2(b). In fact, as indicated by (D.3), the superior outage performance of the proposed RSMA-SGF scheme is achievable without any constraints on the values of ϵ_B and ϵ_F by avoiding the outage floor.

In Fig. 3, we investigate the outage performance achieved by the considered SGF schemes for various transmit power settings. In particular, we assume $P_B = P_F$ in Fig. 3(a) and a fixed transmit power $P_B = 10$ dB in Fig. 3(b), respectively. The curves in Fig. 3(a) also show that the proposed RSMA-SGF scheme achieves the best outage performance without suffering outage floors. In the small and middle transmit SNR regions, the proposed scheme achieves the smaller outage probabilities than those of the PC-SGF scheme. In addition, we can see from Fig. 3(b) that when P_B is fixed at 10 dB, the proposed scheme lowers the outage probability than the QoS-SGF and PC-SGF schemes in the whole transmit SNR region.

In Fig. 4(a), we examine the accuracy of the developed analytical results for the outage probability. In Fig. 4(a), we set $\{\hat{R}_B = 2$ BPCU, $\hat{R}_F = 1.5$ BPCU $\}$ and use the expressions provided by Theorem 1 and Corollary 1 to obtain the analytical results. The curves in Fig. 4(a) show that the developed analytical results match the simulation results perfectly verifying the

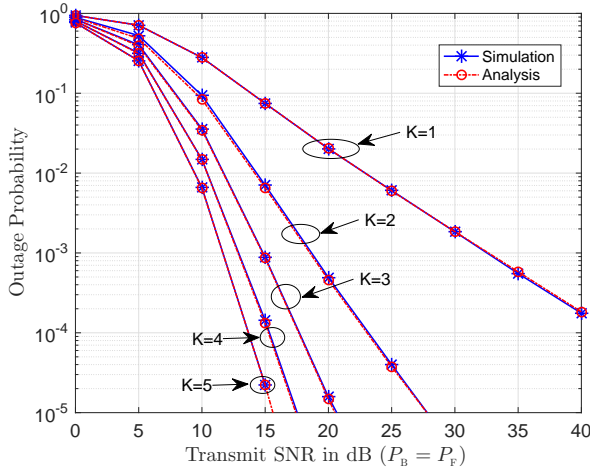


(a) $P_B = P_F$ ($\hat{R}_B = 2$ BPCU and $\hat{R}_F = 1.5$ BPCU)

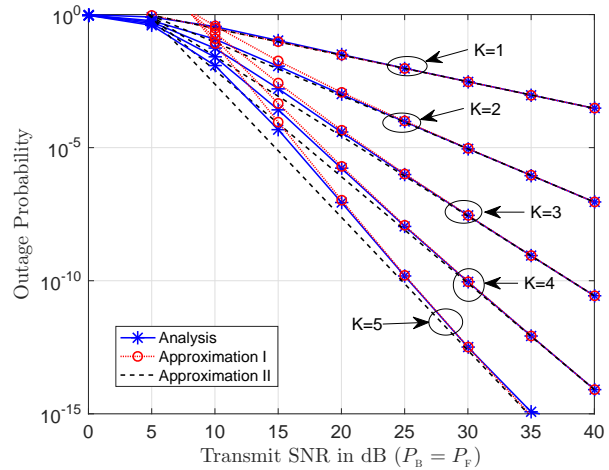


(b) Fixed $P_B = 10$ dB ($\hat{R}_B = 1.5$ BPCU and $\hat{R}_F = 2$ BPCU)

Fig. 3. Outage probability comparison of the SGF schemes for various transmit power settings.



(a) Exact analytical results



(b) Approximation results

Fig. 4. Accuracy of the developed analytical results. The curves for Analysis are based Theorem 1 and Corollary 1, the curves for Approximation I are based on Theorem 2, and the curves for Approximation II are based on Corollary 2 and Corollary 3.

accuracy of the expressions in Theorem 1 and Corollary 1. In Fig. 4(b), we set $\{\hat{R}_B = 1.5$ BPCU, $\hat{R}_F = 2$ BPCU $\}$ and use the developed expression in Theorem 2 to obtain the results for the curves of “Approximation I”. In addition, the developed expressions in Corollary 2 and Corollary 3 are applied to obtain the results for the curves of “Approximation II”. From Fig. 4(b), we can see that the curves of “Approximation I” match well with the analytical results

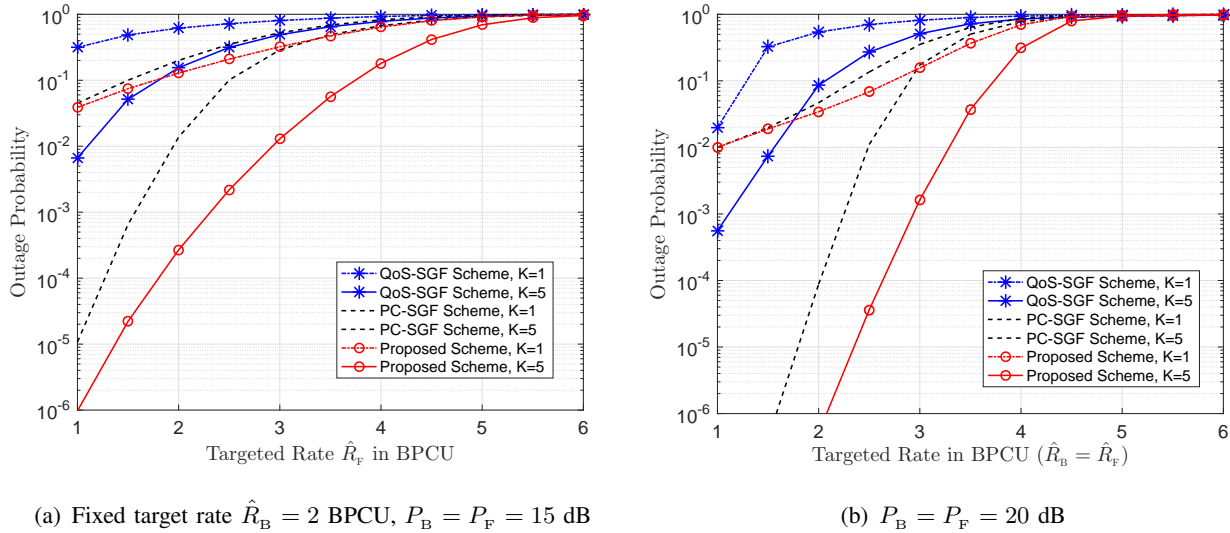


Fig. 5. Impact of the target rate on the outage probability.

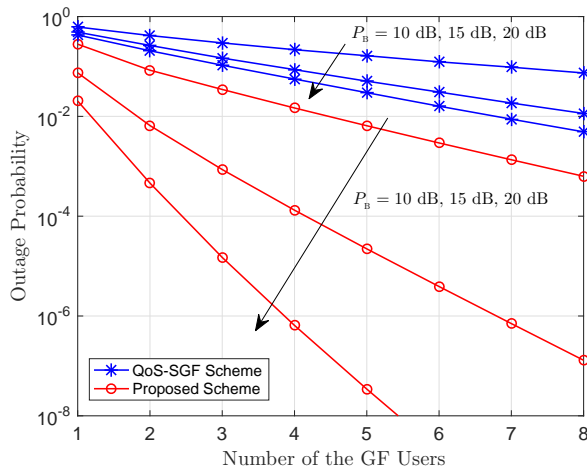


Fig. 6. Impact of the number of the GF users on the outage probability ($\hat{R}_B = 2$ BPCU and $\hat{R}_F = 1.5$ BPCU, and $P_B = P_F$).

in the high SNR region. Furthermore, we can see that the curves of “Approximation I” match well with the analytical results except for the larger values of K . Specifically, as the values of K increase, the gaps between the curves of “Approximation I” and analytical results become larger since we neglect two probability related terms, Q_k ($0 \leq k \leq K - 1$) and Q_{K+1} , in the approximation made for Corollary 2.

The impact of the target rate on the outage probability is investigated in Fig. 5. In particular, we fix $\hat{R}_B = 2$ BPCU for the GB user in Fig. 5(a) and set $\hat{R}_B = \hat{R}_F$ in Fig. 5(b), respectively. It

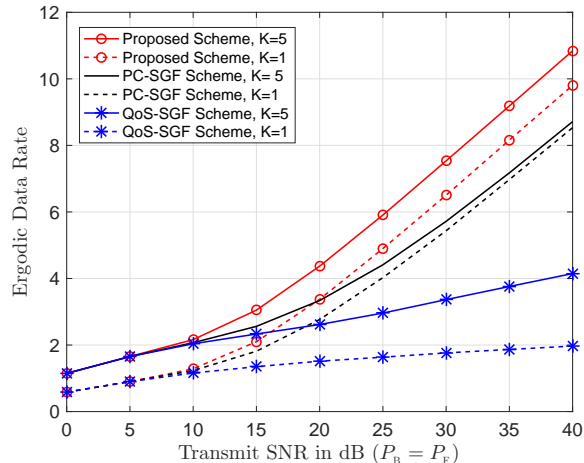


Fig. 7. Ergodic data rate comparison of the SGF schemes ($\hat{R}_B = 4$ BPCU).

is shown in Figs. 5(a) and 5(b) that for the given transmit SNR values, the proposed RSMA-SGF scheme achieves the smallest outage probabilities in the considered whole target rate region. As the target rate increases, the outage probability values achieved by all the SGF schemes increase and approach 1 as the target rate increases.

The impact of the number of the GF users on the outage probability is investigated in Fig. 6, for which we set $\{\hat{R}_B = 2$ BPCU, $\hat{R}_F = 1.5$ BPCU $\}$ and $P_B = P_F$. The results achieved by the QoS-SGF scheme are also provided for comparison. From Fig. 6, the superior outage performance achieved by the RSMA-SGF scheme over that of the QoS-SGF scheme is verified. As K increases, the proposed RSMA-SGF scheme significantly lowers the outage probability owing to multiuser diversity.

In Fig. 7, we evaluate the exact ergodic rate of the considered SGF schemes to verify the superior performance of the proposed RSMA-SGF scheme. It is shown in Fig. 7 that the RSMA-SGF scheme achieves the highest ergodic rate among three SGF schemes. Compared to the QoS-SGF scheme, the curve slope of the RSMA-SGF scheme is much larger, which verifies that RSMA-SGF scheme can exploit multiuser diversity more effectively than the QoS-SGF scheme. In addition, the RSMA-SGF scheme with $K = 1$ even achieves a higher ergodic rate than that of the PC-SGF scheme with $K = 5$ in the high SNR region, which verifies that the RSMA-SGF scheme outperforms the PC-SGF scheme. For considered high target rate $\hat{R}_B = 4$ BPCU, the ergodic rate gap of the PC-SGF scheme between $K = 1$ and $K = 5$ decreases as

the SNR increases, whereas the ergodic rate gap of the RSMA-SGF scheme between $K = 1$ and $K = 5$ is almost constant in the high SNR region, which again verifies the superiority of the RSMA-SGF scheme over the existing NOMA-SGF schemes.

VI. CONCLUSIONS

In this paper, we have proposed an RSMA-SGF scheme to improve the outage performance of SGF transmissions. By applying RS, the RSMA-SGF scheme can effectively use the transmit power to exploit the advantages of power-domain superposition. Without introducing additional interference to the GB user, the proposed RSMA-SGF scheme has significantly improved the reliability of the GF users' transmissions compared to the existing NOMA-SGF schemes. To evaluate the outage performance of the RSMA-SGF scheme, we have derived exact and approximated expressions for the outage probability of the admitted GF user, which revealed that the full multiuser diversity gain is achievable irrespective of the target rate values. Computer simulation results have been provided to clarify the superior outage performance of the proposed RSMA-SGF scheme. As one of the future research topics, user scheduling strategies considering stochastic geometry can be applied to enhance the user fairness of the RSMA-SGF scheme.

APPENDIX A: A PROOF OF THEOREM 1

Since the probability term Q_k involves different order statistics for different k values, we evaluate different Q_k s considering their associated order statistics, respectively.

A. Evaluation of Q_0

The probability term Q_0 can be rewritten as

$$\begin{aligned} Q_0 &= \Pr \left(|h_B|^2 > \eta_B, |h_1|^2 > \frac{P_B \epsilon_B^{-1} |h_B|^2 - 1}{P_F}, |h_K|^2 < \frac{(1 + \epsilon_F)(1 + \epsilon_B) - (1 + P_B |h_B|^2)}{P_F} \right) \\ &= \mathcal{E}_{\eta_B < |h_B|^2 < \eta_B(1 + \epsilon_F) + \frac{\epsilon_F}{P_B}} \{S_0\} \end{aligned} \quad (\text{A.1})$$

where $\mathcal{E}\{\cdot\}$ stands for the expectation operation and S_0 is defined by

$$S_0 \triangleq \Pr \left(|h_1|^2 > \frac{P_B \epsilon_B^{-1} |h_B|^2 - 1}{P_F}, |h_K|^2 < \frac{(1 + \epsilon_F)(1 + \epsilon_B) - (1 + P_B |h_B|^2)}{P_F} \right). \quad (\text{A.2})$$

In (A.1), the expectation for S_0 is taken over $|h_B|^2 < \eta_B(1 + \epsilon_F) + \frac{\epsilon_F}{P_B}$ besides $|h_B|^2 > \eta_B$ due to the constraint $\frac{(1 + \epsilon_F)(1 + \epsilon_B) - (1 + P_B |h_B|^2)}{P_F} > 0$, which is required by the fact that $|h_K|^2$ is positive

in practice. Furthermore, since the upper bound on $|h_K|^2$ should be larger than the lower bound on $|h_1|^2$ in S_0 , the expectation for S_0 should be taken under the following hidden constraint

$$|h_B|^2 < \eta_B(1 + \epsilon_F), \quad (\text{A.3})$$

which is equivalent to $\frac{(1+\epsilon_F)(1+\epsilon_B)-(1+P_B|h_B|^2)}{P_F} > \frac{P_B\epsilon_B^{-1}|h_B|^2-1}{P_F}$. Consequently, the expectation for S_0 should be taken over $\eta_B < |h_B|^2 < \eta_B(1 + \epsilon_F)$ to obtain Q_0 .

Note that the joint probability density function (PDF) of the order statistics $|h_1|^2$ and $|h_K|^2$ is given by

$$f_{|h_1|^2, |h_K|^2}(x, y) = \varphi_0 e^{-x} (e^{-x} - e^{-y})^{K-2} e^{-y} \quad (\text{A.4})$$

with $x < y$ and $\varphi_0 = \frac{K!}{(K-2)!}$, S_0 can be evaluated as follows:

$$\begin{aligned} S_0 &= \varphi_0 \sum_{i=0}^{K-2} \binom{K-2}{i} (-1)^i \int_{\frac{\eta_B^{-1}|h_B|^2-1}{P_F}}^{\frac{(1+\epsilon_F)(1+\epsilon_B)-(1+P_B|h_B|^2)}{P_F}} e^{-(K-i-1)x} \\ &\quad \times \int_x^{\frac{(1+\epsilon_F)(1+\epsilon_B)-(1+P_B|h_B|^2)}{P_F}} e^{-(i+1)y} dy dx \\ &= \varphi_0 \sum_{i=0}^{K-2} \binom{K-2}{i} \frac{(-1)^i}{i+1} \\ &\quad \times \left(\frac{\tilde{\mu}_3 e^{-\tilde{\mu}_4 |h_B|^2} - \tilde{\mu}_5 e^{-\tilde{\mu}_6 |h_B|^2}}{K} - \frac{\tilde{\mu}_1 e^{-\tilde{\mu}_2 |h_B|^2} - \tilde{\mu}_5 e^{-\tilde{\mu}_6 |h_B|^2}}{K-i-1} \right), \end{aligned} \quad (\text{A.5})$$

where $\tilde{\mu}_1 = e^{\frac{K-(1+i)(1+\epsilon_B)(1+\epsilon_F)}{P_F}}$, and $\tilde{\mu}_2 = \frac{K-i-1}{P_F \eta_B} - \frac{P_B(1+i)}{P_F}$, $\tilde{\mu}_3 = e^{\frac{K}{P_F}}$, $\tilde{\mu}_4 = \frac{K}{P_F \eta_B}$, $\tilde{\mu}_5 = e^{-\frac{K(\eta_B + \eta_F + \eta_B \eta_F)}{P_F}}$, and $\tilde{\mu}_6 = -\frac{K P_B}{P_F}$.

In order to facilitate expressing Q_k ($0 \leq k \leq K$), we introduce a general expectation term $\nu(i, \mu)$ as follows:

$$\begin{aligned} \nu(i, \mu) &\triangleq \int_{\eta_B < |h_B|^2 < \eta_B(1+\epsilon_F)} \mathcal{E} \left\{ e^{-\left(\frac{i}{P_F \eta_B} + \mu\right) |h_B|^2} \right\} \\ &= \int_{\eta_B}^{\eta_B(1+\epsilon_F)} e^{-\left(\frac{i}{P_F \eta_B} + \mu + 1\right)x} dx \\ &= \begin{cases} \epsilon_F \eta_B, & \text{if } \mu = -1 - \frac{i}{P_F \eta_B}, \\ \frac{e^{-\eta_B \left(\frac{i}{P_F \eta_B} + \mu + 1\right)} - e^{-\eta_B(1+\epsilon_F) \left(\frac{i}{P_F \eta_B} + \mu + 1\right)}}{\frac{i}{P_F \eta_B} + \mu + 1}, & \text{otherwise.} \end{cases} \end{aligned} \quad (\text{A.6})$$

Applying the results of (A.6) into (A.5), Q_0 can be calculated as

$$Q_0 = \varphi_0 \sum_{i=0}^{K-2} \binom{K-2}{i} \frac{(-1)^i}{i+1} \left(\frac{\tilde{\mu}_3 \nu(0, \tilde{\mu}_4) - \tilde{\mu}_5 \nu(0, \tilde{\mu}_6)}{K} - \frac{\tilde{\mu}_1 \nu(0, \tilde{\mu}_2) - \tilde{\mu}_5 \nu(0, \tilde{\mu}_6)}{K-i-1} \right). \quad (\text{A.7})$$

Since that Q_0 in (A.7) is too complicated to obtain a high SNR approximation, we simplify it in the following way.

By applying $\binom{K-2}{i} = \binom{K-1}{i+1} \frac{i+1}{K-1}$ and substituting $\ell = i+1$ into (A.7), Q_0 can be rewritten as follows:

$$Q_0 = -\frac{\varphi_0}{K-1} \sum_{\ell=0}^{K-1} \binom{K-1}{\ell} (-1)^\ell \left(\frac{\tilde{\mu}_3 \nu(0, \tilde{\mu}_4) - \tilde{\mu}_5 \nu(0, \tilde{\mu}_6)}{K} - \frac{\mu_1 \nu(0, \mu_2) - \tilde{\mu}_5 \nu(0, \tilde{\mu}_6)}{K-\ell} \right), \quad (\text{A.8})$$

where $\mu_1 = e^{\frac{K-\ell(1+\epsilon_B)(1+\epsilon_F)}{P_F}}$ and $\mu_2 = \frac{K-\ell}{P_F \eta_B} - \frac{P_B \ell}{P_F}$. In (A.8), we add the term for $\ell = 0$ without changing the summation value due to the fact that $\frac{\tilde{\mu}_3 \nu(0, \tilde{\mu}_4) - \tilde{\mu}_5 \nu(0, \tilde{\mu}_6)}{K} - \frac{\mu_1 \nu(0, \mu_2) - \tilde{\mu}_5 \nu(0, \tilde{\mu}_6)}{K-\ell} = 0$ when $\ell = 0$. By eliminating the terms that are independent of ℓ based on the fact that $\sum_{\ell=0}^{K-1} \binom{K-1}{\ell} (-1)^\ell = 0$, Q_0 can be simplified as:

$$\begin{aligned} Q_0 &= \frac{\varphi_0}{K-1} \sum_{\ell=0}^{K-1} \binom{K-1}{\ell} (-1)^\ell \frac{\mu_1 \nu(0, \mu_2) - \tilde{\mu}_5 \nu(0, \tilde{\mu}_6)}{K-\ell} \\ &= \frac{\varphi_0}{K(K-1)} \sum_{\ell=0}^K \binom{K}{\ell} (-1)^\ell (\mu_1 \nu(0, \mu_2) - \tilde{\mu}_5 \nu(0, \tilde{\mu}_6)), \end{aligned} \quad (\text{A.9})$$

where the term for $\ell = K$ is added without changing the summation value due to the fact that $\mu_1 \nu(0, \mu_2) - \tilde{\mu}_5 \nu(0, \tilde{\mu}_6) = 0$ when $\ell = K$.

Again, by eliminating the terms that are independent of ℓ based on the fact that $\sum_{\ell=0}^K \binom{K}{\ell} (-1)^\ell = 0$, Q_0 can be further simplified as:

$$Q_0 = \frac{\varphi_0}{K(K-1)} \sum_{\ell=0}^K \binom{K}{\ell} (-1)^\ell \mu_1 \nu(0, \mu_2). \quad (\text{A.10})$$

B. Evaluation of Q_k for $1 \leq k \leq K-2$

When $1 \leq k \leq K-2$, three order statistics, h_k , h_{k+1} , and h_K , are involved in probability Q_k in the form of

$$\begin{aligned} Q_k &= \Pr \left(|h_B|^2 > \eta_B, |h_k|^2 < \frac{\tau}{P_F}, |h_{k+1}|^2 > \frac{\tau}{P_F}, R_{\text{II},K} < \hat{R}_F \right) \\ &= \mathcal{E}_{\eta_B < |h_B|^2 < \eta_B(1+\epsilon_F)} \{S_k\}, \end{aligned} \quad (\text{A.11})$$

where S_k is defined by

$$S_k \triangleq \Pr \left(|h_k|^2 < \frac{P_B \epsilon_B^{-1} |h_B|^2 - 1}{P_F}, |h_{k+1}|^2 > \frac{P_B \epsilon_B^{-1} |h_B|^2 - 1}{P_F} \right),$$

$$|h_K|^2 < \frac{(1 + \epsilon_F)(1 + \epsilon_B) - (1 + P_B |h_B|^2)}{P_F}. \quad (\text{A.12})$$

In (A.11), the expectation is taken over $\eta_B < |h_B|^2 < \eta_B(1 + \epsilon_F)$ considering the relationship between the upper and lower bounds on channel gains.

For the case $1 \leq k \leq K - 2$, the joint PDF of three order statistics, h_k , h_{k+1} , and h_K , is given by

$$\begin{aligned} f_{|h_k|^2, |h_{k+1}|^2, |h_K|^2}(x, y, z) &= \tilde{\varphi}_k e^{-x} (1 - e^{-x})^{k-1} e^{-y} (e^{-y} - e^{-z})^{K-k-2} e^{-z} \\ &= \tilde{\varphi}_k \sum_{i=0}^{K-k-2} \binom{K-k-2}{i} (-1)^i e^{-x} (1 - e^{-x})^{k-1} e^{-(K-k-i-1)y} e^{-(i+1)z}, \end{aligned} \quad (\text{A.13})$$

where $x \leq y \leq z$ and $\tilde{\varphi}_k = \frac{K!}{(k-1)!(K-k-2)!}$. Using the above joint PDF, S_k can be expressed in terms of $|h_B|^2$ as follows:

$$\begin{aligned} S_k &= \tilde{\varphi}_k \sum_{i=0}^{K-k-2} \binom{K-k-2}{i} (-1)^i \int_0^{\frac{\eta_B^{-1} |h_B|^2 - 1}{P_F}} e^{-x} (1 - e^{-x})^{k-1} \\ &\quad \times \int_{\frac{\eta_B^{-1} |h_B|^2 - 1}{P_F}}^{\frac{(1+\epsilon_F)(1+\epsilon_B) - (1+P_B |h_B|^2)}{P_F}} e^{-(K-k-i-1)y} \int_y^{\frac{(1+\epsilon_F)(1+\epsilon_B) - (1+P_B |h_B|^2)}{P_F}} e^{-(i+1)z} dz dy dx. \end{aligned} \quad (\text{A.14})$$

After some algebraic manipulations, S_k can be evaluated as follows:

$$\begin{aligned} S_k &= \tilde{\varphi}_k \sum_{i=0}^{K-k-2} \binom{K-k-2}{i} \sum_{\ell=0}^k \binom{k}{\ell} \frac{(-1)^{\ell+i} e^{\frac{\ell}{P_F}} e^{-\frac{\ell |h_B|^2}{P_F \eta_B}}}{k(i+1)} \\ &\quad \times \left(\frac{\tilde{\mu}_1 e^{-\tilde{\mu}_2 |h_B|^2} - \tilde{\mu}_5 e^{-\tilde{\mu}_6 |h_B|^2}}{K-k} - \frac{\tilde{\mu}_3 e^{-\tilde{\mu}_4 |h_B|^2} - \tilde{\mu}_5 e^{-\tilde{\mu}_6 |h_B|^2}}{K-k-i-1} \right), \end{aligned} \quad (\text{A.15})$$

where $\tilde{\mu}_1 = e^{\frac{K-k}{P_F}}$, $\tilde{\mu}_2 = \frac{K-k}{P_F \eta_B}$, $\tilde{\mu}_3 = e^{\frac{K-k-(1+i)(1+\epsilon_B)(1+\epsilon_F)}{P_F}}$, $\tilde{\mu}_4 = \frac{K-k-i-1}{P_F \eta_B} - \frac{(1+i)P_B}{P_F}$, $\tilde{\mu}_5 = e^{-\frac{(K-k)(\epsilon_B + \epsilon_F + \epsilon_B \epsilon_F)}{P_F}}$, and $\tilde{\mu}_6 = -\frac{(K-k)P_B}{P_F}$.

Taking the expectation for S_k according to (A.11), Q_k can be evaluated as:

$$\begin{aligned} Q_k &= \tilde{\varphi}_k \sum_{i=0}^{K-k-2} \binom{K-k-2}{i} \frac{(-1)^i}{k(i+1)} \sum_{\ell=0}^k \binom{k}{\ell} (-1)^\ell e^{\frac{\ell}{P_F}} \\ &\quad \times \left(\frac{\tilde{\mu}_1 \nu(\ell, \tilde{\mu}_2) - \tilde{\mu}_5 \nu(\ell, \tilde{\mu}_6)}{K-k} - \frac{\tilde{\mu}_3 \nu(\ell, \tilde{\mu}_4) - \tilde{\mu}_5 \nu(\ell, \tilde{\mu}_6)}{K-k-i-1} \right), \end{aligned} \quad (\text{A.16})$$

where $\nu(\ell, \tilde{\mu})$ is given by (A.6). For the expression in (A.16), we can replace $\binom{K-k-2}{i}$ with $\binom{K-k-1}{i+1} \frac{i+1}{K-k-1}$ and let $n = i + 1$, so that Q_k can be rewritten as:

$$Q_k = \frac{-\tilde{\varphi}_k}{k(K-k-1)} \sum_{n=0}^{K-k-1} \binom{K-k-1}{n} (-1)^n \sum_{\ell=0}^k \binom{k}{\ell} (-1)^\ell e^{\frac{\ell}{P_F}}$$

$$\times \left(\frac{\tilde{\mu}_1 \nu(\ell, \tilde{\mu}_2) - \tilde{\mu}_5 \nu(\ell, \tilde{\mu}_6)}{K-k} - \frac{\mu_3 \nu(\ell, \mu_4) - \tilde{\mu}_5 \nu(\ell, \tilde{\mu}_6)}{K-k-n} \right), \quad (\text{A.17})$$

where $\mu_3 = e^{\frac{K-k-n(1+\epsilon_B)(1+\epsilon_F)}{P_F}}$ and $\mu_4 = \frac{K-k-n}{P_F \eta_B} - \frac{n P_B}{P_F}$. For (A.17), we note that the added term for $n = 0$ does not change the value of Q_k due to the fact that $\frac{\tilde{\mu}_1 \nu(\ell, \tilde{\mu}_2) - \tilde{\mu}_5 \nu(\ell, \tilde{\mu}_6)}{K-k} - \frac{\mu_3 \nu(\ell, \mu_4) - \tilde{\mu}_5 \nu(\ell, \tilde{\mu}_6)}{K-k-n} = 0$ when $n = 0$.

Furthermore, some terms in (A.17) involving $\tilde{\mu}_1$, $\tilde{\mu}_2$, $\tilde{\mu}_5$, and $\tilde{\mu}_6$ but being independent of n can be further eliminated due to the fact that $\sum_{n=0}^k \binom{k}{n} (-1)^n = 0$, while $\tilde{\mu}_1$, $\tilde{\mu}_2$, $\tilde{\mu}_5$, and $\tilde{\mu}_6$ are not functions of n . The simplification can be expressed as follows:

$$\begin{aligned} Q_k &= \frac{\tilde{\varphi}_k}{k(K-k-1)} \sum_{n=0}^{K-k-1} \binom{K-k-1}{n} (-1)^n \sum_{\ell=0}^k \binom{k}{\ell} (-1)^\ell e^{\frac{\ell}{P_F}} \frac{\mu_3 \nu(\ell, \mu_4) - \tilde{\mu}_5 \nu(\ell, \tilde{\mu}_6)}{K-k-n} \\ &\stackrel{(a)}{=} \varphi_k \sum_{n=0}^{K-k} \binom{K-k}{n} (-1)^n \sum_{\ell=0}^k \binom{k}{\ell} (-1)^\ell e^{\frac{\ell}{P_F}} (\mu_3 \nu(\ell, \mu_4) - \tilde{\mu}_5 \nu(\ell, \tilde{\mu}_6)) \\ &\stackrel{(b)}{=} \varphi_k \sum_{n=0}^{K-k} \binom{K-k}{n} (-1)^n \sum_{\ell=0}^k \binom{k}{\ell} (-1)^\ell e^{\frac{\ell}{P_F}} \mu_3 \nu(\ell, \mu_4), \end{aligned} \quad (\text{A.18})$$

where step (a) follows by absorbing $K-k-1$ into the binomial coefficients without changing the summation value and step (b) follows by using the fact that $\sum_{n=0}^k \binom{k}{n} (-1)^n = 0$ while $\tilde{\mu}_5$ and $\tilde{\mu}_6$ are not functions of n .

C. Evaluation of Q_{K-1}

$$\begin{aligned} Q_{K-1} &= \mathcal{E}_{|h_B|^2 > \eta_B} \left\{ \Pr \left(|h_{K-1}|^2 < \frac{P_B \epsilon_B^{-1} |h_B|^2 - 1}{P_F}, |h_K|^2 > \frac{P_B \epsilon_B^{-1} |h_B|^2 - 1}{P_F} \right. \right. \\ &\quad \left. \left. |h_K|^2 < \frac{(1+\epsilon_F)(1+\epsilon_B) - (1+P_B |h_B|^2)}{P_F} \right) \right\} \end{aligned} \quad (\text{A.19})$$

By extracting the hidden constraint on the upper and lower bounds on $|h_K|^2$ from (A.19), i.e., $\frac{P_B \epsilon_B^{-1} |h_B|^2 - 1}{P_F} < \frac{(1+\epsilon_F)(1+\epsilon_B) - (1+P_B |h_B|^2)}{P_F}$, Q_{K-1} can be rewritten as follows:

$$Q_{K-1} = \mathcal{E}_{\eta_B < |h_B|^2 < (1+\epsilon_F)\eta_B} \{S_{K-1}\}, \quad (\text{A.20})$$

where S_{K-1} denotes probability inside the expectation in (A.19). There are two order statistics h_{K-1} and h_K involving in S_{K-1} with their joint PDF being given by

$$f_{|h_{K-1}|^2, |h_K|^2}(x, y) = \varphi_0 e^{-x} (1 - e^{-x})^{K-2} e^y, \quad (\text{A.21})$$

where $x \leq y$. With the aid of this joint PDF, S_{K-1} can be evaluated as follows:

$$S_{K-1} = \varphi_0 \sum_{\ell=0}^{K-1} \binom{K-1}{\ell} \frac{(-1)^\ell e^{\frac{\ell}{P_F}} e^{-\frac{\ell|h_B|^2}{P_F \eta_B}}}{K-1} \left(e^{\frac{1}{P_F}} e^{-\mu_5 |h_B|^2} - e^{-\frac{\epsilon_B + \epsilon_F + \epsilon_B \epsilon_F}{P_F}} e^{-\mu_6 |h_B|^2} \right), \quad (\text{A.22})$$

where $\mu_5 = \frac{1}{P_F \eta_B}$ and $\mu_6 = -\frac{P_B}{P_F}$. By using the results in (A.6), Q_{K-1} can be derived as follows:

$$Q_{K-1} = \frac{\varphi_0}{K-1} \sum_{\ell=0}^{K-1} \binom{K-1}{\ell} (-1)^\ell e^{\frac{\ell}{P_F}} \left(e^{\frac{1}{P_F}} \nu(\ell, \mu_5) - e^{-\frac{\epsilon_B + \epsilon_F + \epsilon_B \epsilon_F}{P_F}} \nu(\ell, \mu_6) \right). \quad (\text{A.23})$$

D. Evaluation of Q_K and Q_{K+1}

In the case of Q_K , the determination of the probability value involves two independent random variables $|h_B|^2$ and $|h_K|^2$. Recalling the expression in (11), Q_K can be rewritten as follows:

$$Q_K = \mathcal{E}_{|h_B|^2 > \eta_B} \left\{ \Pr \left(|h_K|^2 < \frac{\eta_B^{-1} |h_B|^2 - 1}{P_F}, |h_K|^2 < \frac{\epsilon_F}{P_F} \right) \right\}. \quad (\text{A.24})$$

Comparing $\frac{\eta_B^{-1} |h_B|^2 - 1}{P_F}$ and $\frac{\epsilon_F}{P_F}$, it can be shown that $\frac{\eta_B^{-1} |h_B|^2 - 1}{P_F} < \frac{\epsilon_F}{P_F}$ if $|h_B|^2 < \eta_B(1 + \epsilon_F)$; otherwise, $\frac{\eta_B^{-1} |h_B|^2 - 1}{P_F} > \frac{\epsilon_F}{P_F}$. Therefore, Q_K can be evaluated as follows:

$$\begin{aligned} Q_K &= \mathcal{E}_{\eta_B < |h_B|^2 < \eta_B(1+\epsilon_F)} \left\{ \Pr \left(|h_K|^2 < \frac{\eta_B^{-1} |h_B|^2 - 1}{P_F} \right) \right\} + \mathcal{E}_{|h_B|^2 > \eta_B(1+\epsilon_F)} \left\{ \Pr (|h_K|^2 < \eta_F) \right\} \\ &= \int_{\eta_B}^{\eta_B(1+\epsilon_F)} \left(1 - e^{-\frac{\eta_B^{-1} x - 1}{P_F}} \right)^K e^{-x} dx + (1 - e^{-\eta_F})^K e^{-\eta_B(1+\epsilon_F)} \\ &= \sum_{\ell=0}^K \binom{K}{\ell} (-1)^\ell e^{\frac{\ell}{P_F}} \int_{\eta_B}^{\eta_B(1+\epsilon_F)} e^{-\left(\frac{\ell}{P_F \eta_B} + 1\right)x} dx + (1 - e^{-\eta_F})^K e^{-\eta_B(1+\epsilon_F)} \\ &= \sum_{\ell=0}^K \binom{K}{\ell} (-1)^\ell e^{\frac{\ell}{P_F}} \nu(\ell, 0) + (1 - e^{-\eta_F})^K e^{-\eta_B(1+\epsilon_F)} \end{aligned} \quad (\text{A.25})$$

Similarly to Q_K , Q_{K+1} is a function of two independent random variables $|h_B|^2$ and $|h_K|^2$. Recalling that $R_{\text{II},K} = \log_2 \left(1 + \frac{P_F |h_K|^2}{P_B |h_B|^2 + 1} \right)$ when $\tau = 0$ occurs, Q_{K+1} can be evaluated as follows:

$$\begin{aligned} Q_{K+1} &= \Pr \left(|h_B|^2 < \eta_B, \log_2 \left(1 + \frac{P_F |h_K|^2}{P_B |h_B|^2 + 1} \right) < \hat{R}_F \right) \\ &= \sum_{\ell=0}^K \binom{K}{\ell} (-1)^\ell e^{-\ell \eta_F} \frac{1 - e^{-(1+\ell \eta_F P_B) \eta_B}}{1 + \ell \eta_F P_B}. \end{aligned} \quad (\text{A.26})$$

APPENDIX B: A PROOF OF THEOREM 2

Regarding that Q_k depends on the value of k , the high SNR approximations for different Q_k will be tackled separately in the following subsections.

A. High SNR approximation for Q_0

Based on the derived closed-form expression in (A.10), Q_0 can be rewritten as follows:

$$\begin{aligned} Q_0 &= \frac{\varphi_0}{K(K-1)} \sum_{\ell=0}^K \binom{K}{\ell} (-1)^\ell \mu_1 \nu(0, \mu_2). \\ &= \frac{\varphi_0}{K(K-1)} \sum_{\ell=0}^K \binom{K}{\ell} (-1)^\ell \mu_1 \int_{\eta_B}^{\eta_B(1+\epsilon_F)} e^{-(\mu_2+1)x} dx \end{aligned} \quad (\text{B.1})$$

By applying the approximation, $e^{-x} = 1 - x$ for $x \rightarrow 0$, and using the definitions of μ_1 and μ_2 , Q_0 can be approximated as follows:

$$\begin{aligned} Q_0 &= \frac{\varphi_0}{K(K-1)} \int_{\eta_B}^{\eta_B(1+\epsilon_F)} \sum_{\ell=0}^K \binom{K}{\ell} (-1)^\ell e^{-\frac{\ell(1+\epsilon_B)(1+\epsilon_F)}{P_F}} e^{\ell(\epsilon_B^{-1}+1)x} dx \\ &\stackrel{(a)}{=} \frac{\varphi_0}{K(K-1)} \int_{\eta_B}^{\eta_B(1+\epsilon_F)} \left(1 - e^{-\left(\frac{(1+\epsilon_B)(1+\epsilon_F)}{P_F} - (\epsilon_B^{-1}+1)x\right)} \right)^K dx \\ &= \frac{\varphi_0}{K(K-1)} \int_{\eta_B}^{\eta_B(1+\epsilon_F)} \left(\frac{(1+\epsilon_B)(1+\epsilon_F)}{P_F} - (\epsilon_B^{-1}+1)x \right)^K dx, \end{aligned} \quad (\text{B.2})$$

where step (a) is obtained by using the fact that $\sum_{\ell=0}^K \binom{K}{\ell} (-1)^\ell a^\ell = (1-a)^K$. By applying the binomial expansion, Q_0 can be further simplified as follows:

$$\begin{aligned} Q_0 &= \frac{\varphi_0}{K(K-1)} \sum_{\ell=0}^K \binom{K}{\ell} \left(\frac{(1+\epsilon_B)(1+\epsilon_F)}{P_F} \right)^{K-\ell} (-1)^\ell (\epsilon_B^{-1}+1)^\ell \int_{\eta_B}^{\eta_B(1+\epsilon_F)} x^\ell dx \\ &= \frac{\varphi_0 \epsilon_B (1+\epsilon_B)^K}{P_F^{K+1} K(K-1)} \sum_{\ell=0}^K \binom{K}{\ell} \frac{(-1)^\ell}{\ell+1} \left((1+\epsilon_F)^{K+1} - (1+\epsilon_F)^{K-\ell} \right). \end{aligned} \quad (\text{B.3})$$

B. High SNR approximation for Q_k with $1 \leq k \leq K-2$

Recalling the results in Appendix A, Q_k can be rewritten as follows:

$$Q_k = \varphi_k \sum_{n=0}^{K-k} \binom{K-k}{n} (-1)^n \sum_{\ell=0}^k \binom{k}{\ell} (-1)^\ell e^{\frac{\ell}{P_F}} \mu_3 \int_{\eta_B}^{\eta_B(1+\epsilon_F)} e^{-\left(\frac{\ell}{P_F \eta_B} + \mu_4 + 1\right)x} dx. \quad (\text{B.4})$$

By applying the approximation $e^{-x} \approx 1 - x$ for $x \rightarrow 0$ and using the definitions of μ_3 and μ_4 , Q_k can be approximated as follows:

$$\begin{aligned} Q_k &= \varphi_k \sum_{n=0}^{K-k} \binom{K-k}{n} (-1)^n \sum_{\ell=0}^k \binom{k}{\ell} (-1)^\ell e^{\frac{\ell}{P_F}} e^{-\frac{n(1+\epsilon_B)(1+\epsilon_F)}{P_F}} \\ &\quad \times \int_{\eta_B}^{\eta_B(1+\epsilon_F)} e^{-\left(\frac{\ell}{P_F \eta_B} - \frac{n}{P_F \eta_B} - n\right)x} dx. \end{aligned} \quad (\text{B.5})$$

By using the fact that $\sum_{\ell=0}^k \binom{k}{\ell} (-1)^\ell a^\ell = (1-a)^k$, the above Q_k can be expressed as follows:

$$\begin{aligned}
Q_k &= \varphi_k \int_{\eta_B}^{\eta_B(1+\epsilon_F)} \sum_{n=0}^{K-k} \binom{K-k}{n} (-1)^n \sum_{\ell=0}^k \binom{k}{\ell} (-1)^\ell \\
&\quad \times e^{-n \left(\frac{(1+\epsilon_B)(1+\epsilon_F)}{P_F} - (\epsilon_B^{-1}+1)x \right)} e^{-\ell(\epsilon_B^{-1}x - P_F^{-1})} dx \\
&= \varphi_k \int_{\eta_B}^{\eta_B(1+\epsilon_F)} \left(1 - e^{-\left(\frac{(1+\epsilon_B)(1+\epsilon_F)}{P_F} - (\epsilon_B^{-1}+1)x \right)} \right)^{K-k} \left(1 - e^{-(\epsilon_B^{-1}x - P_F^{-1})} \right)^k dx \\
&\stackrel{(a)}{=} \varphi_k \int_{\eta_B}^{\eta_B(1+\epsilon_F)} \left(\frac{(1+\epsilon_B)(1+\epsilon_F)}{P_F} - (\epsilon_B^{-1}+1)x \right)^{K-k} (\epsilon_B^{-1}x - P_F^{-1})^k dx, \tag{B.6}
\end{aligned}$$

where step (a) follows high SNR approximations. Applying the binomial expansions to (B.6), the high SNR approximation for Q_k can be obtained as follows:

$$\begin{aligned}
Q_k &= \frac{\varphi_k \epsilon_B (1+\epsilon_B)^{K-k} (-1)^k}{P_F^{K+1}} \sum_{n=0}^{K-k} \binom{K-k}{n} (-1)^n (1+\epsilon_F)^{K-k-n} \\
&\quad \times \sum_{\ell=0}^k \binom{k}{\ell} (-1)^\ell \frac{(1+\epsilon_F)^{n+\ell+1} - 1}{n+\ell+1}. \tag{B.7}
\end{aligned}$$

C. High SNR approximation for Q_{K-1}

First, we rewrite Q_{K-1} as follows:

$$\begin{aligned}
Q_{K-1} &= \frac{\varphi_0}{K-1} \sum_{\ell=0}^{K-1} \binom{K-1}{\ell} (-1)^\ell e^{\frac{\ell}{P_F}} \left(e^{\frac{1}{P_F}} \nu(\ell, \mu_5) - e^{-\frac{\epsilon_B + \epsilon_F + \epsilon_B \epsilon_F}{P_F}} \nu(\ell, \mu_6) \right) \\
&= \frac{\varphi_0}{K-1} \sum_{\ell=0}^{K-1} \binom{K-1}{\ell} (-1)^\ell e^{\frac{\ell}{P_F}} \int_{\eta_B}^{\eta_B(1+\epsilon_F)} \left(e^{\frac{1}{P_F}} e^{-\left(\frac{\ell}{P_F \eta_B} + \mu_5 + 1 \right)x} \right. \\
&\quad \left. - e^{-\frac{\epsilon_B + \epsilon_F + \epsilon_B \epsilon_F}{P_F}} e^{-\left(\frac{\ell}{P_F \eta_B} + \mu_6 + 1 \right)x} \right) dx. \tag{B.8}
\end{aligned}$$

By using the fact that $\sum_{\ell=0}^k \binom{k}{\ell} (-1)^\ell = 0$, Q_{K-1} can be expressed as follows:

$$Q_{K-1} = \frac{\varphi_0}{K-1} \int_{\eta_B}^{\eta_B(1+\epsilon_F)} \left(e^{\frac{1}{P_F} - (\epsilon_B^{-1}+1)x} - e^{-\frac{\epsilon_B + \epsilon_F + \epsilon_B \epsilon_F}{P_F}} \right) \left(1 - e^{-\ell(\epsilon_B^{-1}x - P_F^{-1})} \right)^{K-1} dx \tag{B.9}$$

By applying the approximations $e^{-x} = 1 - x$ for $x \rightarrow 0$, Q_{K-1} can be approximated as follows:

$$\begin{aligned}
Q_{K-1} &= \frac{\varphi_0}{K-1} \int_{\eta_B}^{\eta_B(1+\epsilon_F)} \left(\frac{(1+\epsilon_B)(1+\epsilon_F)}{P_F} - (\epsilon_B^{-1}+1)x \right) (\epsilon_B^{-1}x - P_F^{-1})^{K-1} dx \\
&= \frac{\varphi_0}{K-1} \int_{\eta_B}^{\eta_B(1+\epsilon_F)} \epsilon_B^{-(K-1)} \left(\frac{(1+\epsilon_B)(1+\epsilon_F)}{P_F} - (\epsilon_B^{-1}+1)x \right) \left(x - \frac{\epsilon_B}{P_F} \right)^{K-1} dx
\end{aligned}$$

$$\begin{aligned}
&= \frac{\varphi_0}{K-1} \int_{\eta_B}^{\eta_B(1+\epsilon_F)} \epsilon_B^{-(K-1)} \frac{(1+\epsilon_B)(1+\epsilon_F)}{P_F} \left(x - \frac{\epsilon_B}{P_F}\right)^{K-1} dx \\
&\quad - \frac{\varphi_0}{K-1} \int_{\eta_B}^{\eta_B(1+\epsilon_F)} \epsilon_B^{-(K-1)} (\epsilon_B^{-1} + 1)x \left(x - \frac{\epsilon_B}{P_F}\right)^{K-1} dx \\
&= \frac{\varphi_0 \epsilon_B \epsilon_F^K (1+\epsilon_B)(1+\epsilon_F)}{P_F^{K+1} K(K-1)} - \frac{\varphi_0 \epsilon_F^K (\epsilon_B^{-1} + 1)(K(1+\epsilon_F) + 1)}{P_F^{K+1} K(K-1)(K+1)}. \tag{B.10}
\end{aligned}$$

Following similar procedures as for deriving the approximation of Q_k ($1 \leq k \leq K-1$), Q_K and Q_{K+1} can be approximated as

$$Q_K = \frac{\epsilon_B \epsilon_F^{K+1}}{P_F^{K+1}(K+1)} + \frac{\epsilon_F^K}{P_F^K} - \frac{\epsilon_B \epsilon_F^K (1+\epsilon_F)}{P_F^{K+1}} \tag{B.11}$$

and

$$Q_{K+1} = \frac{\epsilon_F^K ((1+\epsilon_B)^{K+1} - 1)}{P_F^{K+1}(K+1)} - \frac{\epsilon_F^K ((\epsilon_B(K+1) - 1)(1+\epsilon_B)^{K+1} + 1)}{P_F^{K+2}(K+2)(K+1)}, \tag{B.12}$$

respectively.

By combing (B.3), (B.7), (B.10), (B.11), and (B.12), the high SNR approximation for P_{out} is obtained.

APPENDIX C: A PROOF OF COROLLARY 3

Recalling the expression in (14), the outage probability experienced by the single GF user can be rewritten as follows:

$$\begin{aligned}
P_{\text{out}} &= \mathcal{E}_{\eta_B < |h_B|^2 < \eta_B(1+\epsilon_F)} \left\{ \Pr \left(|h_1|^2 < \frac{(1+\epsilon_F)(1+\epsilon_B) - (1+P_B|h_B|^2)}{P_F} \right) \right\} \\
&\quad + \mathcal{E}_{|h_B|^2 > \eta_B(1+\epsilon_F)} \left\{ \Pr \left(|h_1|^2 < \frac{\epsilon_F}{P_F} \right) \right\} + \mathcal{E}_{|h_B|^2 < \eta_B} \left\{ \Pr \left(|h_1|^2 < \frac{\epsilon_F(1+P_B|h_B|^2)}{P_F} \right) \right\}. \tag{C.1}
\end{aligned}$$

By using the approximation $1 - e^{-x} = x$ for $x \rightarrow 0$, the high SNR approximation for the outage probability can be calculated as follows:

$$\begin{aligned}
P_{\text{out}} &\approx \int_{\eta_B}^{\eta_B(1+\epsilon_F)} \frac{e^{-x}(\epsilon_B + \epsilon_F + \epsilon_B \epsilon_F - P_B x)}{P_F} dx + \int_{\eta_B(1+\epsilon_F)}^{\infty} \frac{\epsilon_F e^{-x}}{P_F} dx \\
&\quad + \int_0^{\eta_B} \frac{\epsilon_F e^{-x}(1+P_B|h_B|^2)}{P_F} dx \\
&\stackrel{(a)}{\approx} \frac{\epsilon_B \epsilon_F (\epsilon_F - \epsilon_B)}{P_F^2} + \frac{\epsilon_F}{P_F} - \frac{\epsilon_B \epsilon_F (1+\epsilon_F)}{P_F^2} + \frac{\epsilon_B \epsilon_F (1+\epsilon_B)}{P_F^2} \\
&= \frac{\epsilon_F}{P_F}, \tag{C.2}
\end{aligned}$$

where step (a) is obtained by using the approximation $1 - e^{-x} = x$ for $x \rightarrow 0$ again.

APPENDIX D: A PROOF OF COROLLARY 4

By using (9), an upper bound of the outage probability achieved by the RSMA-SGF scheme can be obtained as follows:

$$\begin{aligned}
P_{\text{out}} &= \Pr\left(E_0, R_{\text{II},K} < \hat{R}_F\right) + \sum_{k=1}^{K-1} \Pr\left(E_k, R_{\text{II},K} < \hat{R}_F\right) + \Pr\left(E_K, R_{\text{I},K} < \hat{R}_F\right) \\
&\leq \sum_{k=0}^{K-1} \underbrace{\Pr\left(|h_K|^2 > \frac{\tau}{P_F}, R_{\text{II},K} < \hat{R}_F\right)}_{Q_F} + \Pr\left(R_{\text{I},K} < \hat{R}_F\right) \\
&= KQ_F + \Pr\left(|h_K|^2 < \frac{\epsilon_F}{P_F}\right). \tag{D.1}
\end{aligned}$$

By using the definitions of τ and $R_{\text{II},K}$, Q_F can be rewritten as follows:

$$Q_F = \Pr\left(|h_K|^2 > \frac{P_B \epsilon_B^{-1} |h_B|^2 - 1}{P_F}, |h_K|^2 < \frac{(1 + \epsilon_F)(1 + \epsilon_B) - (1 + P_B |h_B|^2)}{P_F}\right). \tag{D.2}$$

Obviously, the lower bound on $|h_K|^2$, i.e., $\frac{P_B \epsilon_B^{-1} |h_B|^2 - 1}{P_F}$, needs to be smaller than the corresponding upper bound, i.e., $\frac{(1 + \epsilon_F)(1 + \epsilon_B) - (1 + P_B |h_B|^2)}{P_F}$, which introduces a hidden constraint

$$|h_B|^2 < \eta_B(1 + \epsilon_F). \tag{D.3}$$

Since the expression in (D.3) does not require any additional constraint on ϵ_B and ϵ_F , Q_F can be evaluated as follows:

$$\begin{aligned}
Q_F &= \Pr\left(|h_K|^2 > \frac{P_B \epsilon_B^{-1} |h_B|^2 - 1}{P_F}, |h_K|^2 < \frac{(1 + \epsilon_F)(1 + \epsilon_B) - (1 + P_B |h_B|^2)}{P_F}, \right. \\
&\quad \left. |h_B|^2 < \eta_B(1 + \epsilon_F)\right) \\
&\leq \Pr(|h_B|^2 < \eta_B(1 + \epsilon_F)) = 1 - e^{-\frac{\epsilon_B(1 + \epsilon_F)}{P_F}} \xrightarrow{P_B \rightarrow \infty} 0, \tag{D.4}
\end{aligned}$$

where the last inequality indicates that the constraint $|h_B|^2 < \eta_B(1 + \epsilon_F)$ effectively removes the outage floor. On the other hand, the remaining term $\Pr\left(|h_K|^2 < \frac{\epsilon_F}{P_F}\right)$ in (D.1) also approaches zero in the high SNR region. Therefore, without requiring any additional constraint on the target rate values (equivalently ϵ_B and ϵ_F), P_{out} does not experience an outage floor in the RSMA-SGF scheme.

REFERENCES

- [1] “Roadmap for IoT research, innovation and development in Europe,” EU NGIoT, Jan. 2020.
- [2] L. Liu, E. G. Larsson, W. Yu, P. Popovski, C. Stefanovic, and E. de Carvalho, “Sparse signal processing for grant-free massive connectivity: A future paradigm for random access protocols in the internet of things,” *IEEE Signal Process. Mag.*, vol. 35, no. 5, pp. 88–99, Sept. 2018.
- [3] A. Bayesteh, E. Yi, H. Nikopour, and H. Baligh, “Blind detection of SCMA for uplink grant-free multiple-access,” in *Proc. Int. Symp. Wireless Commun. Systems (ISWCS)*, Barcelona, Spain, 26–29 Aug. 2014, pp. 1–6.
- [4] M. Yang, B. Li, Z. Bai, and Z. Yan, “SGMA: Semi-granted multiple access for non-orthogonal multiple access (NOMA) in 5G networking,” *J. Netw. Comput. Appl.*, vol. 112, no. Mar., pp. 115–125, 2018.
- [5] Z. Ding, R. Schober, P. Fan, and H. V. Poor, “Simple semi-grant-free transmission strategies assisted by non-orthogonal multiple access,” *IEEE Trans. Commun.*, vol. 67, no. 6, pp. 4464–4478, Jun. 2019.
- [6] Z. Ding, R. Schober, and H. V. Poor, “A new QoS-guarantee strategy for NOMA assisted semi-grant-free transmission,” *IEEE Trans. Commun.*, pp. 1–30, In Press, 2021.
- [7] C. Zhang, Z. Qin, Y. Liu, and K. K. Chai, “Semi-grant-free uplink NOMA with contention control: A stochastic geometry model,” in *Proc. 2020 IEEE Int. Conf. Commun. Works.*, Dublin, Ireland, 7–11 Jun. 2020, pp. 1–6.
- [8] H. Lu, X. Xie, Z. Shi, H. Lei, H. Yang, and J. Cai, “Advanced NOMA assisted semi-grant-free transmission schemes for randomly distributed users,” *arXiv:2012.09423*, pp. 1–35, 2020. [Online]. Available: <https://arxiv.org/abs/2012.09423>
- [9] Z. Yang, P. Xu, J. Ahmed Hussein, Y. Wu, Z. Ding, and P. Fan, “Adaptive power allocation for uplink non-orthogonal multiple access with semi-grant-free transmission,” *IEEE Wireless Commun. Lett.*, vol. 9, no. 10, pp. 1725–1729, Oct. 2020.
- [10] Z. Ding, R. Schober, and H. V. Poor, “Unveiling the importance of SIC in NOMA systems—Part I: State of the art and recent findings,” *IEEE Commun. Lett.*, vol. 24, no. 11, pp. 2378–2382, Nov. 2020.
- [11] C. Zhang, Y. Liu, Z. Qin, and Z. Ding, “Semi-grant-free NOMA: A stochastic geometry model,” *arXiv:2006.13286*, pp. 1–14, 2020. [Online]. Available: <https://arxiv.org/abs/2006.13286>
- [12] N. Jayanth, P. Chakraborty, M. Gupta, and S. Prakriya, “Performance of semi-grant free uplink with non-orthogonal multiple access,” in *Proc. IEEE Int. Symp. Pers. Indoor Mob. Radio Commun.*, London, UK, 31 Aug.–3 Sept. 2020, pp. 1–6.
- [13] D. Pliatsios, A.-A. A. Boulogeorgos, T. Lagkas, V. Argyriou, I. D. Moscholios, and P. Sarigiannidis, “Semi-grant-free non-orthogonal multiple access for tactile internet of things,” in *Proc. IEEE Int. Symp. Pers. Indoor Mob. Radio Commun.*, Helsinki, Finland, 13–16 Sept. 2021, pp. 1–6.
- [14] C. Zhang, Y. Liu, W. Yi, Z. Qin, and Z. Ding, “Semi-grant-free noma: Ergodic rates analysis with random deployed users,” *IEEE Wireless Commun. Lett.*, vol. 10, no. 4, pp. 692–695, April 2021.
- [15] M. Fayaz, W. Yi, Y. Liu, and A. Nallanathan, “Competitive MA-DRL for transmit power pool design in semi-grant-free NOMA systems,” *arXiv:2106.11190*, 2021. [Online]. Available: <https://arxiv.org/abs/2106.11190>
- [16] B. Rimoldi and R. Urbanke, “A rate-splitting approach to the Gaussian multiple-access channel,” *IEEE Trans. Inf. Theory*, vol. 42, no. 2, pp. 364–375, Mar. 1996.
- [17] H. Liu, T. A. Tsiftsis, K. J. Kim, K. S. Kwak, and H. V. Poor, “Rate splitting for asynchronous uplink NOMA systems with cyclic prefixed single carrier,” in *Proc. 2019 IEEE International Conference on Communications Workshops (ICC Workshops)*, Shanghai, China, 20–24 May, 2019, pp. 1–6.
- [18] H. Liu, T. A. Tsiftsis, K. J. Kim, K. S. Kwak, and H. V. Poor, “Rate splitting for uplink NOMA with enhanced fairness and outage performance,” *IEEE Trans. Wireless Commun.*, vol. 19, no. 7, pp. 4657–4670, Jul. 2020.

- [19] J. Zeng, T. Lv, W. Ni, R. Liu, N. C. Beaulieu, and Y. J. G. Fan, "Ensuring max-min fairness of UL SIMO-NOMA: A rate splitting approach," *IEEE Trans. Veh. Technol.*, vol. 68, no. 11, pp. 11 080–11 093, Nov. 2019.
- [20] Z. Yang, M. Chen, W. Saad, W. Xu, and M. Shikh-Bahaei, "Sum-rate maximization of uplink rate splitting multiple access (RSMA) communication," *IEEE Trans. Mobile Comput.*, pp. 1–14, 2020.
- [21] W. Jaafar, S. Naser, S. Muhaidat, P. C. Sofotasios, and H. Yanikomeroglu, "Multiple access in aerial networks: From orthogonal and non-orthogonal to rate-splitting," *IEEE Open J. Veh. Technol.*, vol. 1, pp. 372–392, Oct. 2020.
- [22] Q. Zhao and L. Tong, "Opportunistic carrier sensing for energy-efficient information retrieval in sensor networks," *EURASIP J. Wireless Commun. Networking*, vol. 2, no. 2, pp. 231–241, Apr. 2005.
- [23] A. Bletsas, A. Khisti, D. P. Reed, and A. Lippman, "A simple cooperative diversity method based on network path selection," *IEEE J. Sel. Areas Commun.*, vol. 24, no. 3, pp. 659–672, Mar. 2006.
- [24] R. Talak and N. B. Mehta, "Feedback overhead-aware, distributed, fast, and reliable selection," *IEEE Trans. Commun.*, vol. 60, no. 11, pp. 3417–3428, Nov. 2012.